ANTI-FLU THERAPY

Universal protection against influenza infection by a multidomain antibody to influenza hemagglutinin

Nick S. Laursen[1]*, Robert H. E. Friesen[2]†, Xueyong Zhu[1], Mandy Jongeneelen[3], Sven Blokland[3], Jan Vermond[4], Alida van Eijgen[4], Chan Tang[3], Harry van Diepen[4], Galina Obmolova[2], Marijn van der Neut Kolfschoten[3], David Zuijdgeest[3], Roel Straetemans[5], Ryan M. B. Hoffman[1], Travis Nieusma[1], Jesper Pallesen[1], Hannah L. Turner[1], Steffen M. Bernard[1], Andrew B. Ward[1], Jinquan Luo[2], Leo L. M. Poon[6], Anna P. Tretiakova[7]‡, James M. Wilson[7], Maria P. Limberis[7], Ronald Vogels[3], Boerries Brandenburg[3], Joost A. Kolkman[8]§, Ian A. Wilson[1,9]§

Broadly neutralizing antibodies against highly variable pathogens have stimulated the design of vaccines and therapeutics. We report the use of diverse camelid single-domain antibodies to influenza virus hemagglutinin to generate multidomain antibodies with impressive breadth and potency. Multidomain antibody MD3606 protects mice against influenza A and B infection when administered intravenously or expressed locally from a recombinant adeno-associated virus vector. Crystal and single-particle electron microscopy structures of these antibodies with hemagglutinins from influenza A and B viruses reveal binding to highly conserved epitopes. Collectively, our findings demonstrate that multidomain antibodies targeting multiple epitopes exhibit enhanced virus cross-reactivity and potency. In combination with adeno-associated virus–mediated gene delivery, they may provide an effective strategy to prevent infection with influenza virus and other highly variable pathogens.

Seasonal influenza epidemics cause worldwide morbidity and mortality (*1*), whereas the vast reservoir of influenza A viruses in aquatic birds represents continual pandemic threats (*2*–*4*). Vaccines remain essential for influenza prevention, but their efficacy is substantially reduced in the elderly, who are at increased risk of influenza-related complications (*3*, *5*, *6*). Annual selection of vaccine strains presents many challenges, and a poor match with circulating viruses can result in suboptimal effectiveness (*7*). Moreover, most vaccine-induced antibodies are directed against the highly variable head region of hemagglutinin (HA) and are strain specific. However, broadly neutralizing antibodies (bnAbs) targeting influenza HA have been isolated and characterized (*8*). Several bnAbs have entered clinical trials as therapeutic agents, but their use in influenza prophylaxis remains elusive because of the incomplete coverage against circulating human influenza A and B viruses, which necessitates administration of a bnAb cocktail, and the need for multiple, high-dose injections for protection throughout the entire influenza season. High serum bnAb levels are required because of poor distribution to the upper airways. We present an alternative strategy for long-lasting protection in which single-domain antibodies (sdAbs) (*9*) with influenza A or B reactivity are linked together into a multidomain antibody (MDAb) and expressed at the nasopharyngeal mucosa through the intranasal administration of a recombinant adeno-associated virus (AAV) vector (*10*, *11*) encoding the MDAb transgene.

Broadly neutralizing sdAbs were obtained by immunizing llamas with influenza vaccine and H7 and H2 recombinant HA (rHA) (*12*). HA cross-reactive sdAbs were isolated from the sdAb [the single variable domain of a heavy-chain-only camelid antibody (V_HH)] repertoires of the immunized llamas by phage display with various cross-selection strategies on rHAs from different influenza subtypes. We isolated two influenza A (SD36 and SD38) and two influenza B (SD83 and SD84) sdAbs and analyzed their in vitro neutralizing activity (Fig. 1). SD36 potently neutralized influenza A group 2 (H3, H4, H7, and

[1]Department of Integrative Structural and Computational Biology, The Scripps Research Institute, 10550 North Torrey Pines Road, La Jolla, CA 92037, USA. [2]Janssen Research and Development, Spring House, PA 19002, USA. [3]Janssen Vaccines and Prevention, Archimedesweg 4-6, 2333 CN, Leiden, Netherlands. [4]Janssen Prevention Center, Archimedesweg 6, 2333 CN, Leiden, Netherlands. [5]Quantitative Sciences, Janssen Pharmaceutical Companies of Johnson and Johnson, Turnhoutseweg 30, 2340 Beerse, Belgium. [6]Center of Influenza Research and School of Public Health, The University of Hong Kong, Hong Kong SAR, China. [7]Gene Therapy Program, Department of Medicine, University of Pennsylvania, Philadelphia, PA 19104, USA. [8]Janssen Infectious Diseases, Turnhoutseweg 30, 2340, Beerse, Belgium. [9]Skaggs Institute for Chemical Biology, The Scripps Research Institute, 10550 North Torrey Pines Road, La Jolla, CA 92037, USA.
*Present address: Department of Molecular Biology and Genetics, Aarhus University, Gustav Wieds Vej 10, 8000 Aarhus C, Denmark. †Present address: Ablynx, a Sanofi company, Technologiepark 21, 9052 Zwijnaarde, Belgium. ‡Present address: Pfizer, Rare Disease Research Unit, 610 Main Street, Cambridge, MA 02139, USA.
§Corresponding author. Email: wilson@scripps.edu (I.A.W.); jkolkman@its.jnj.com (J.A.K.)

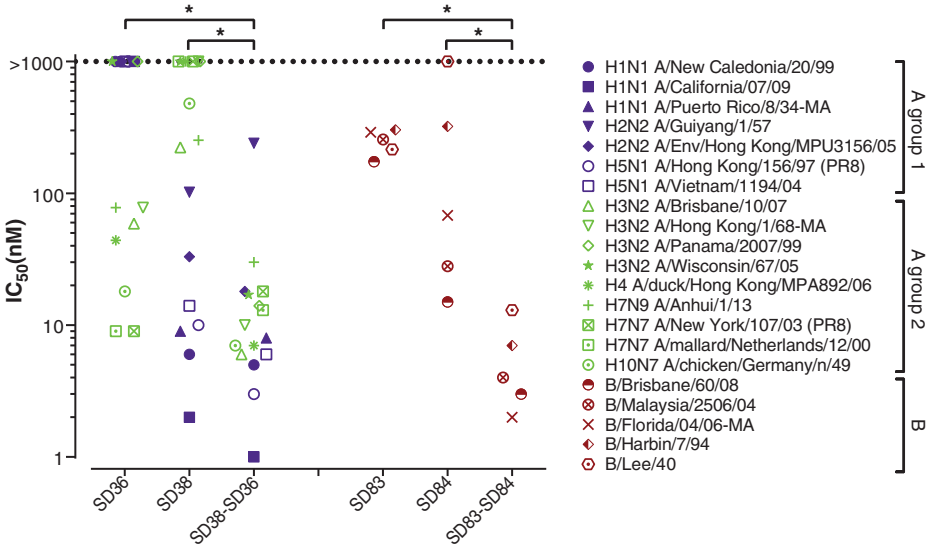

Fig. 1. In vitro neutralization of influenza A and B viruses by individual and genetically fused sdAbs. In vitro potencies of SD36, SD38, SD83, and SD84 and genetically fused sdAbs SD38-SD36 and SD83-SD84 against selected influenza A and B viruses. Both SD38-SD36 and SD83-SD84 are significantly more potent (*$P < 0.05$) than each of their individual components (comparisons are shown via brackets) (see materials and methods in the supplementary materials). Data are representative of at least three independent experiments performed in quadruplicate.

Downloaded from http://science.sciencemag.org/ on April 15, 2021

H10) but not group 1 (H1, H2, and H5) viruses, whereas SD38 potently neutralized group 1 (H1, H2, and H5) and some group 2 (H3, H7, and H10) viruses, albeit with lower potency. SD84 and SD83 neutralized representative viruses from both influenza B lineages.

To elucidate the molecular basis for the broad HA recognition, we determined the crystal structures of SD38 and SD83 to 2.0-Å resolution; SD36, SD38, and SD83 with different HAs to 2.2 to 2.8 Å; humanized SD84 (SD84h) to 0.94 Å; and SD84h with HA (B/Brisbane/60/08) and bnAb CR9114 to 4.1 Å (*13*) (Fig. 2 and table S1). A cryo–electron microscopy (EM) reconstruction of SD84 with B/Massachusetts/02/12 HA and CR9114 was determined to 7.1-Å resolution (fig. S1). All sdAbs except SD84 recognized the HA stem, with three sdAbs bound per trimer (Fig. 2). SD83 contacted conserved residues in the fusion subdomain (Fig. 2A), with complementarity-determining region 2 (CDR2) and CDR3 framing the epitope consisting of HA1 residues 30 to 32, Lys^{45}, Asp^{291}, Asn^{301}, and Pro^{305}; the HA2 A helix; and N-linked glycans at Asn^{301} and Asn^{330} (Fig. 2A). The SD83 epitope was highly conserved, with all contact residues being >99% identical in influenza B viruses (Fig. 2A and table S2). SD83 buried a relatively small surface area (588 Å^2) on HA, which potentially presented fewer possibilities for escape. In contrast, SD84 bound a conserved epitope in the HA head around the receptor binding site (Fig. 2B and table S2). SD36 and SD38 also recognized conserved epitopes that partially overlap with influenza A stem epitopes of bnAbs CR9114, CR6261, and FI6v3 and, to a lesser extent, those of CR8043 and CR8020 (*13*–*16*). SD36 CDR2 and CDR3 contacted the HA2 A helix, HA1 Asn^{291} and Thr^{318}, and HA1 Arg^{32} of the adjacent protomer (Fig. 2C and fig. S2). CDR1 and CDR3 interacted with HA2 residues 19 and 20, and Framework2 (FR2) interacted with HA1 Lys^{54} and Glu^{278}. In SD38, the 17-residue CDR3 dominated and bound to a shallow groove formed by the HA2 A helix, HA2 residues 18 to 21, and HA1 His^{38} and Thr^{318} (Fig. 2D and figs. S2 and S3) (*17*).

Thus, SD38 and SD36 made extensive contacts to the A helix and other highly conserved residues (tables S3 and S4). However, 33% of H3 viruses had an Asp^{46}→Asn (D46N) polymorphism and were not neutralized by SD36 (table S5). Asn^{46} would disrupt a salt bridge and hydrogen bond network with SD36 (fig. S4). SD36 bound H1 HA (A/Brisbane/59/07) with a 290 nM dissociation constant (K_d) (table S6) but did not neutralize the corresponding virus in vitro [median inhibitory concentration

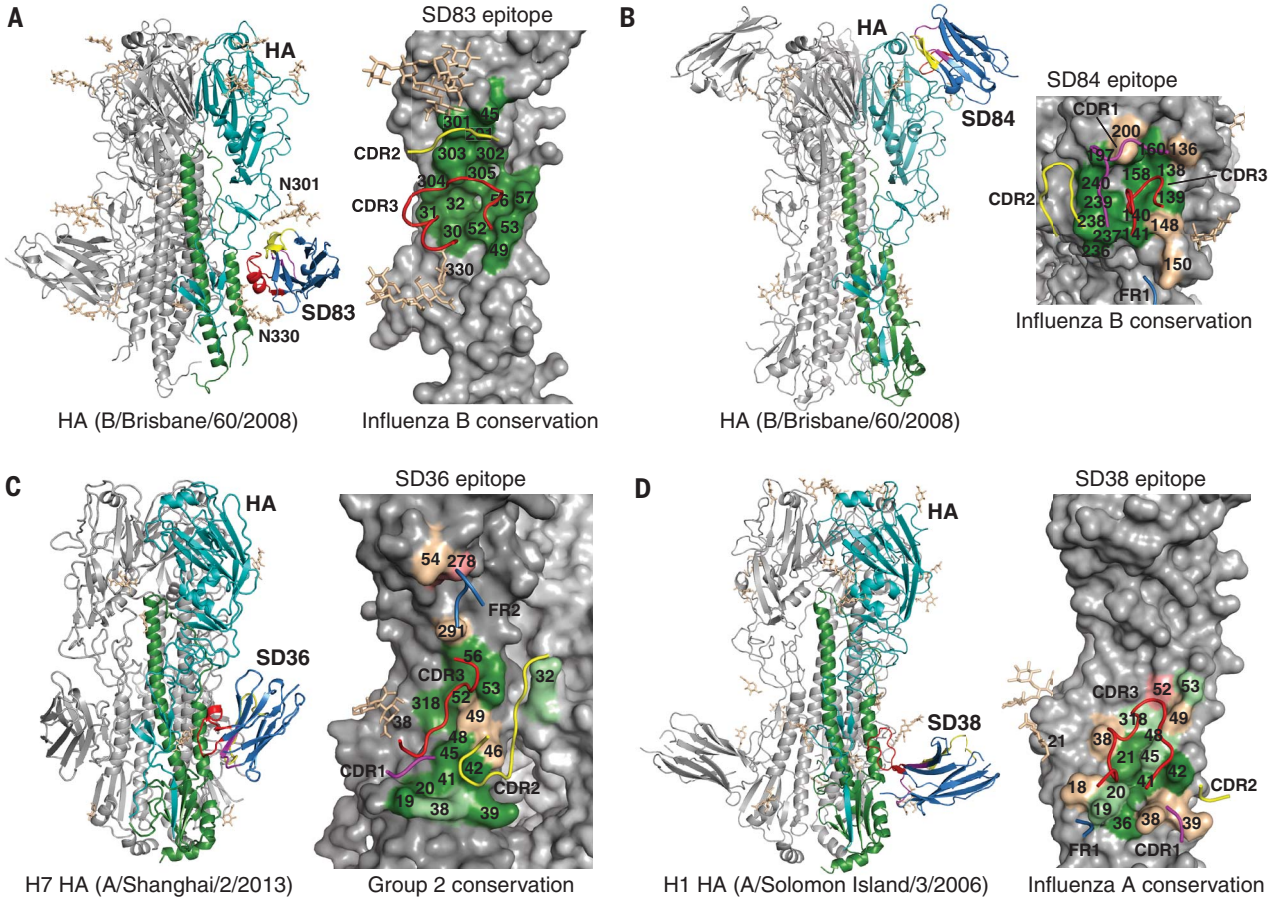

Fig. 2. Crystal structures of sdAbs in complex with HAs and conservation of their epitopes. (**A**) Crystal structure of SD83 with influenza B HA (B/Brisbane/60/08) at 2.2-Å resolution. One HA-SD83 protomer of the trimeric complex is colored with HA1 in cyan, HA2 in green, and SD83 in blue (left). CDR1 is colored in magenta, CDR2 in yellow, and CDR3 in red. The other HA protomers are colored in gray. N-linked glycans are shown in beige in stick representation. The epitope of SD83 is mapped onto the influenza B HA and colored by conservation across influenza B HAs (right). Only the CDR loops involved in the interaction are shown. N301 and N330, Asn^{301} and Asn^{330}. (**B**) Crystal structure of SD84h with influenza B HA (B/Brisbane/60/08) as well as with CR9114 Fab at 4.1-Å resolution (left). The epitope of SD84h is mapped onto the influenza B HA and colored by conservation across influenza B HAs (right). For clarity, CR9114 Fab, which binds to the conserved HA stem region, is not shown. (**C**) Crystal structure of SD36 with H7 HA (A/Shanghai/2/13) at 2.65-Å resolution (left). The epitope of SD36 is mapped onto the H7 HA and colored by conservation across influenza A group 2 HAs (right). (**D**) Crystal structure of SD38 with H1 HA (A/Solomon Islands/3/06) at 2.8-Å resolution (left). The epitope of SD38 is mapped onto the H1 HA and colored by conservation across influenza A HAs (right). For all panels, conservation color coding is as follows: dark green, >95% conserved; light green, 75 to 95% conserved; beige, 50 to 75% conserved; and pink, 35 to 50% conserved.

Downloaded from http://science.sciencemag.org/ on April 15, 2021

(IC_{50}) >1 μM]. As all group 1 viruses were glycosylated at HA1 N289, steric hindrance may have lowered the SD36 affinity below the neutralization threshold, whereas SD38 avoided this glycan (table S6). HA2 Val^{18} and Leu^{38} on the SD38 epitope periphery were the least conserved across H1 strains (table S3 and Fig. 2D), but natural mutations Gln^{38} or Ile^{18} and Gln^{38} did not affect neutralization (table S7).

We next rationalized that linking different sdAbs could generate MDAbs with increased potency and breadth. Thus, MDAbs were engineered by genetically fusing individual sdAbs with peptide linkers and then linking them to human immunoglobulin G1 (IgG1) Fc (Fig. 3). The SD38-SD36 fusion was generally more potent, with broader cross-reactivity, than SD36 and SD38 alone, especially against H3 viruses (Fig. 1). Notably, SD38-SD36 neutralized D46N-carrying H3N2 viruses A/Panama/2007/99 and A/Wisconsin/67/05, neither of which was neutralized by SD36 or SD38, thereby demonstrating a synergistic effect (table S8). SD83-SD84 also neutralized influenza B viruses much more potently, especially B/Lee/40 (Fig. 1). Notably, MD2407 (SD38-SD36-SD83-SD84) and MD3606 (MD2407 fused to human IgG1 Fc) neutralized all A (H1 to H12 and H14) and B viruses tested except for one avian H12 virus (*18*) and had much greater breadth and potency than the individual sdAbs or CR9114 (Fig. 3 and table S9). MD3606 also strongly bound avian H13, H15, and H16 and bat H17 and H18 HAs (table S6).

Depending on their epitopes, known bnAbs inhibit influenza infection by blocking viral attachment, HA proteolytic activation, membrane fusion, or viral egress (*19*–*21*). The HA head–binding SD84 and both MDAbs inhibited hemagglutination by influenza B (B/Florida/04/06-MA) virus (table S10). All three stem binders and both MDAbs blocked the low-pH HA rearrangements required for membrane fusion (fig. S5). Unlike CR8020, the sdAbs or MDAbs could not prevent HA proteolytic activation (HA0 to HA1 and HA2), reflecting their epitope location further up the HA stem (figs. S2 and S6). In contrast to SD83 and SD84, MD2407 and MD3606 inhibited egress of B/Malaysia/2506/04 virus (fig. S7), similar to some other bnAbs (*21*, *22*).

A shift from monovalency (Fab) to bivalency (IgG) can considerably increase the binding and neutralization breadth of influenza A antibodies, mainly to the HA head (*23*–*25*). We extended this concept with our MDAbs that targeted different HA conserved epitopes, resulting in greatly increased potency and unparalleled neutralization breadth. From our crystal and EM structures, we were able to exclude simultaneous binding of the MDAbs to epitopes on the same HA trimer (fig. S8A and table S11) (*26*). MDAbs could also increase avidity through cross-linking adjacent HA trimers on the viral surface. Inter–cross-linked HA complexes (85 to 96 Å) were indeed visible in negative-stain EM (fig. S8B). If this holds for HA trimers on the viral surface, it could partially explain the increased potency of MD2407 and MD3606 versus their individual sdAb components.

To assess in vivo protection, we compared the prophylactic efficacy of MD3606 with that of CR9114 and CR8071 in BALB/c mice challenged with H1N1, H3N2, H7N9, and B viruses by using intravenous administration (Fig. 4, A to D, and figs. S9 and S10). MD3606 at 1.7 mg per kilogram of body weight completely protected mice from a lethal dose of mouse-adapted H1N1 virus (A/Puerto Rico/8/34-MA) and was superior to CR9114 at 5 mg/kg. MD3606 at 5 mg/kg provided complete protection from H3N2 virus (A/Hong Kong/1/68-MA) infection, whereas at 1.7 mg/kg, seven of eight mice survived with MD3606, compared with five of eight with CR9114. With an H7N9 virus (A/Anhui/1/13), mice were completely protected with MD3606 at 5 mg/kg versus 15 mg/kg for CR9114. Finally, at 1 mg/kg, MD3606 protected all mice from influenza B virus (B/Florida/4/06-MA) infection and was superior to CR9114 and CR8071 (12.5 and 50% survival). MD3606 administered 1 day before challenge with H1N1 or B virus also resulted in a dose-dependent reduction in lung viral load (fig. S11).

Antibody-dependent cellular cytotoxicity (ADCC) can also contribute to in vivo bnAb efficacy (*27*). In an ADCC reporter assay, MD3606 activated FcγRIIIa similarly to CR9114 (fig. S12). MD3606 with a murine IgG2a (mIgG2a) Fc protected all mice from lethality with influenza B virus (B/Florida/4/06-MA) at 1 mg/kg intravenously (iv), similar to MD3606 with human IgG1 Fc (fig. S13). A human IgG1 LALA Fc mutant, which decreases binding to human and mouse Fcγ receptors (FcγRs), resulted in 37.5% survival at 1 mg/kg (iv) but 100% survival at 5 mg/kg. MD3606 with a mIgG2aσ Fc domain lacking FcγR binding (*28*) provided full protection at 5 mg/kg but none at 1 mg/kg. These FcγR-mediated effector functions will most likely extend to influenza A viruses, as binding of MD3606 to cells expressing H3 HA (A/Wisconsin/67/05) induced ADCC in vitro (fig. S12).

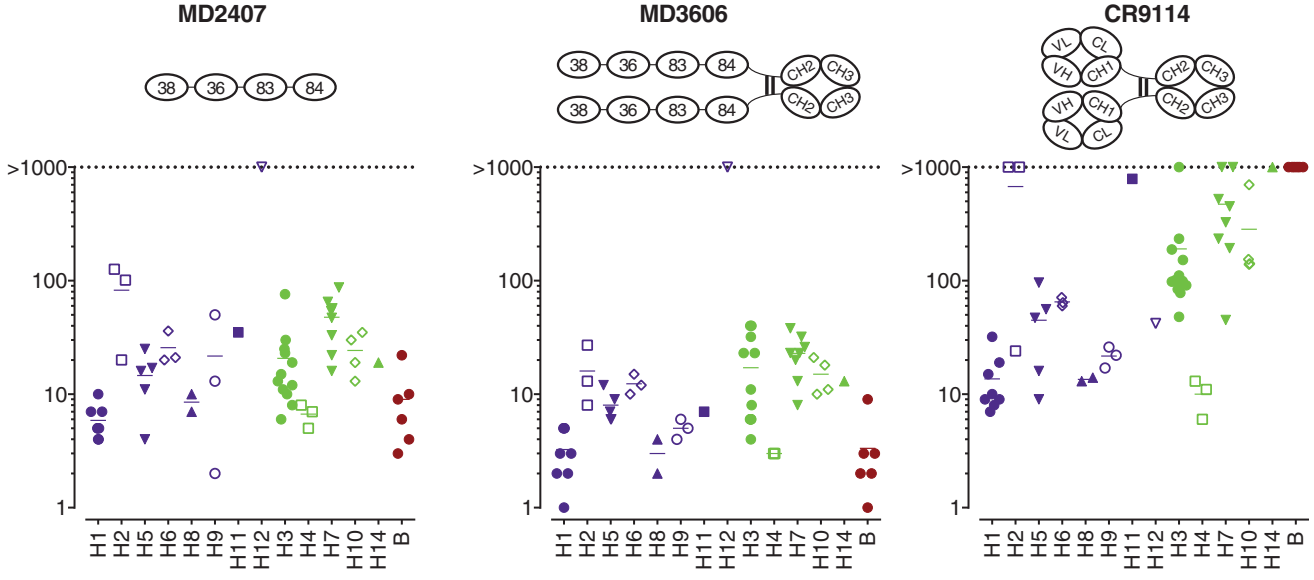

Fig. 3. In vitro neutralization of influenza A and B viruses by pan-influenza MDAbs MD2407 and MD3606 versus CR9114. In vitro potencies of MD2407, MD3606, and CR9114 against a panel of 60 influenza A group 1 (blue), A group 2 (green), and B (red) viruses. A list of the influenza virus strains tested, together with their IC_{50} values, is compiled in table S9. Both MD3606 and MD2407 are significantly more potent ($P < 0.05$) than CR9114 (see materials and methods in the supplementary materials). Data are representative of at least three independent experiments performed in quadruplicate. V_H, variable region of immunoglobulin heavy chain; C_H, constant region of immunoglobulin heavy chain; C_L, constant region of immunoglobulin light chain; V_L, variable region of immunoglobulin light chain.

Downloaded from http://science.sciencemag.org/ on April 15, 2021

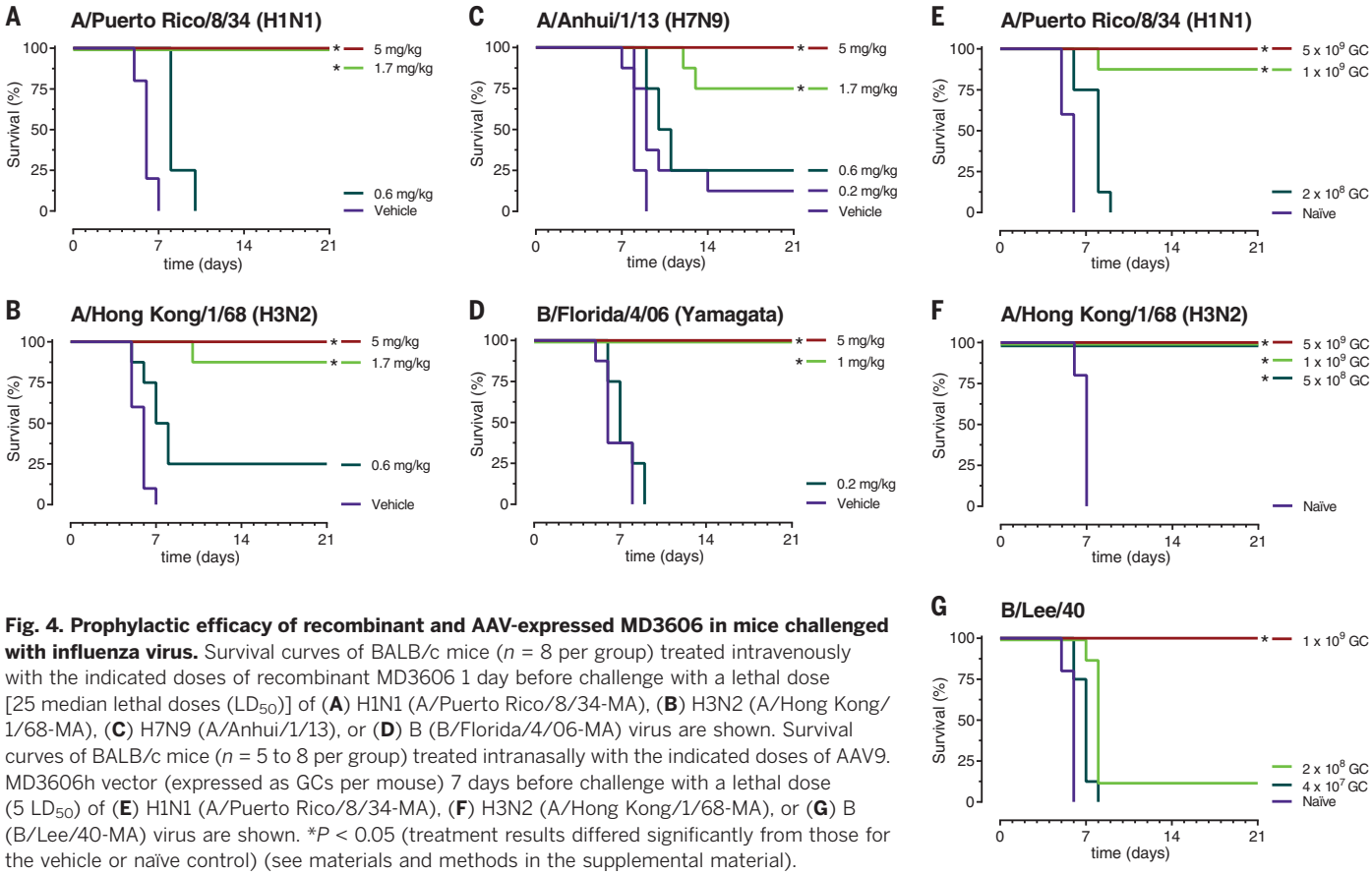

Fig. 4. Prophylactic efficacy of recombinant and AAV-expressed MD3606 in mice challenged with influenza virus. Survival curves of BALB/c mice (n = 8 per group) treated intravenously with the indicated doses of recombinant MD3606 1 day before challenge with a lethal dose [25 median lethal doses (LD_{50})] of (**A**) H1N1 (A/Puerto Rico/8/34-MA), (**B**) H3N2 (A/Hong Kong/1/68-MA), (**C**) H7N9 (A/Anhui/1/13), or (**D**) B (B/Florida/4/06-MA) virus are shown. Survival curves of BALB/c mice (n = 5 to 8 per group) treated intranasally with the indicated doses of AAV9.MD3606h vector (expressed as GCs per mouse) 7 days before challenge with a lethal dose (5 LD_{50}) of (**E**) H1N1 (A/Puerto Rico/8/34-MA), (**F**) H3N2 (A/Hong Kong/1/68-MA), or (**G**) B (B/Lee/40-MA) virus are shown. *P < 0.05 (treatment results differed significantly from those for the vehicle or naïve control) (see materials and methods in the supplemental material).

We then evaluated the prophylactic efficacy of a recombinant AAV9 vector encoding humanized MD3606 (*29*) (AAV9.MD3606h) in mice challenged with mouse-adapted influenza H1N1, H3N2, and B viruses (Fig. 4, E to G, and fig. S14). AAV9.MD3606h was administered intranasally 7 days before influenza challenge at vector doses ranging from 4×10^7 to 5×10^9 genome copies (GCs) per mouse. A dose of 5×10^9 GCs completely protected against lethal challenge with H1N1 virus (A/Puerto Rico/8/34-MA), whereas seven of eight mice survived with a dose of 1×10^9 GCs. Mice challenged with H3N2 (A/Hong Kong/1/68-MA) and B (B/Lee/40-MA) viruses were fully protected by intranasal administration of 5×10^8 GCs (the lowest dose tested) and 1×10^9 GCs, respectively. AAV9.MD3606h also conferred protection against H1N1 virus when administered 35 days before challenge (fig. S15). Preexisting serum-circulating AAV9-specific neutralizing antibodies did not affect the prophylactic efficacy of AAV9.MD3606h (fig. S16).

Limitations of seasonal influenza vaccines, together with the constant threat of a new influenza pandemic, have spurred the search for new influenza prevention strategies. One such strategy involves passive immunization by AAV-mediated delivery of genes encoding protective bnAbs (*11*). In preclinical mouse models, intranasal delivery of AAV9 encoding bnAb FI6 provided protection against H1N1 infection 3 days after vector administration (*11*). Notably, old and immunodeficient mice were also protected from a lethal H1N1 dose (*10*). Mucosal expression of the AAV9 transgene is durable [>9 months in mice (*30*) and 4 months in rhesus macaques (*11*)], and AAV9 vectors can be readministered in the airway without loss of efficiency (*30*). To be clinically useful, AAV-encoded bnAbs should neutralize both influenza A and B viruses, but all bnAbs to date lack sufficient influenza A and B cross-reactivity; the limited AAV packaging capacity (<5 kb) also precludes the expression of two individual bnAbs or a bispecific bnAb from a single vector. We used an alternative antibody platform with camelid-derived sdAbs to create two highly potent MDAbs, MD3606 and MD2407, which have near-universal activity against influenza A and B viruses and can both be expressed from a single AAV vector. Fc-containing MD3606 administered intravenously was more effective than state-of-the-art bnAb CR9114 against seasonal and pandemic influenza viruses, with a significant effect (P < 0.05) on survival in H7N9 and B models (table S12). Intranasal delivery of AAV9.MD3606h provided full protection in mice at doses as low as 5×10^8 GCs. If the above preclinical findings translate to humans, an annual intranasal administration of AAV9.MD3606h may provide passive protection for the entire influenza season and would be of particular benefit to the elderly and other high-risk groups. The rapid onset of protection, together with the unprecedented cross-reactivity of MD3606 to avian influenza strains, also offers the possibility of using this approach as a prophylactic immediately upon onset of an influenza pandemic, providing substantial advantages over vaccination.

REFERENCES AND NOTES

1. World Health Organization (WHO), http://www.who.int/mediacentre/factsheets/fs211/en.
2. J. Liu *et al.*, *Science* **309**, 1206 (2005).
3. H. Chen *et al.*, *Nature* **436**, 191–192 (2005).
4. R. Gao *et al.*, *N. Engl. J. Med.* **368**, 1888–1897 (2013).
5. M. T. Osterholm, N. S. Kelley, A. Sommer, E. A. Belongia, *Lancet Infect. Dis.* **12**, 36–44 (2012).
6. W. E. Beyer *et al.*, *Vaccine* **31**, 6030–6033 (2013).
7. H. Xie *et al.*, *Sci. Rep.* **5**, 15279 (2015).
8. N. C. Wu, I. A. Wilson, *J. Mol. Biol.* **429**, 2694–2709 (2017).
9. S. Krah *et al.*, *Immunopharmacol. Immunotoxicol.* **38**, 21–28 (2016).
10. V. S. Adam *et al.*, *Clin. Vaccine Immunol.* **21**, 1528–1533 (2014).
11. M. P. Limberis *et al.*, *Sci. Transl. Med.* **5**, 187ra72 (2013).
12. See supplementary materials.
13. C. Dreyfus *et al.*, *Science* **337**, 1343–1348 (2012).
14. D. Corti *et al.*, *Science* **333**, 850–856 (2011).
15. D. C. Ekiert *et al.*, *Science* **324**, 246–251 (2009).
16. J. Sui *et al.*, *Nat. Struct. Mol. Biol.* **16**, 265–273 (2009).
17. CDR1 and CDR2 also made minor contacts to the A helix.
18. H12 HA has more mutations in the SD38 epitope than other HA subtypes, including those at HA1 residue 318 (Ile) and HA2 residues 48 (Met), 49 (Gln), and 52 (Leu), which are not present in other subtypes (table S3). However, MD2407 binds H12 HA in biolayer interferometry experiments but with fast on and fast off rates and a K_d value of >550 nM for the first of two sites in a 2:1 binding model, which is higher than those for other subtypes. Further studies will be needed to find out which H12 HA mutation(s) is responsible for the lack of neutralization and whether these resistance mutations can

Downloaded from http://science.sciencemag.org/ on April 15, 2021

emerge in HAs of human influenza viruses (e.g., H1N1 or H3N2) upon treatment with MD3606.
19. J. P. Julien, P. S. Lee, I. A. Wilson, *Immunol. Rev.* **250**, 180–198 (2012).
20. N. S. Laursen, I. A. Wilson, *Antiviral Res.* **98**, 476–483 (2013).
21. B. Brandenburg *et al.*, *PLOS ONE* **8**, e80034 (2013).
22. G. S. Tan *et al.*, *J. Virol.* **88**, 13580–13592 (2014).
23. P. S. Lee *et al.*, *Proc. Natl. Acad. Sci. U.S.A.* **109**, 17040–17045 (2012).
24. A. Hultberg *et al.*, *PLOS ONE* **6**, e17665 (2011).
25. D. C. Ekiert *et al.*, *Nature* **489**, 526–532 (2012).
26. The 10-residue linkers in MD2407 were too short to allow SD36 and SD38, or SD84 and SD83, to bind the same HA trimer (fig. S8A). Furthermore, the potency of SD38-SD36 with an 18-residue linker was indistinguishable from that of constructs with 38- or 60-residue linkers, which should be more permissive for intratrimer binding (table S11).
27. D. J. DiLillo, G. S. Tan, P. Palese, J. V. Ravetch, *Nat. Med.* **20**, 143–151 (2014).
28. O. Vafa *et al.*, *Methods* **65**, 114–126 (2014).
29. Humanization of the four sdAb components of MD3606 (SD36, SD38, SD83, and SD84) is described in patent application WO/2016/124768 (Janssen Vaccines and Prevention, 2016). The humanized sdAbs share 92 to 98% of their framework identity with the closest human V_H germline sequences. Wild-type and humanized MD3606 were virtually indistinguishable in in vitro neutralization assays using different influenza A and B viruses.
30. M. P. Limberis, J. M. Wilson, *Proc. Natl. Acad. Sci. U.S.A.* **103**, 12993–12998 (2006).

ACKNOWLEDGMENTS

We thank N. van Dijk for performing label-free binding assays, W. Yu for protein purification, H. Tien for automated crystal screening, and the staff of the Gene Therapy Program for their invaluable assistance with AAV-directed gene transfer studies. This is publication 29558 from The Scripps Research Institute. **Funding:** This work is supported in part by NIH grants R56 AI117675 and R56 AI127371 (to I.A.W.), by a grant from Janssen, and in part by the Defense Advanced Research Projects Agency, Department of Defense (grant 64047-LS-DRP.02 to J.M.W.) and the Theme-based Research Scheme, Research Grants Council of the Hong Kong (ref. T11-705/14N). X-ray diffraction data were collected at the Advanced Photon Source (APS) beamlines 23ID-B, 23ID-D, and 17-ID and at the Stanford Synchrotron Radiation Lightsource (SSRL) BL12-2. Use of the APS was supported by the U.S. Department of Energy (DOE), Basic Energy Sciences, Office of Science, under contract DE-AC02-06CH11357. GM/CA CAT is funded in whole or in part with federal funds from the National Cancer Institute (Y1-CO-1020) and the NIGMS (Y1-GM-1104). Use of the SSRL, SLAC National Accelerator Laboratory, is supported by the U.S. DOE, Office of Science, Office of Basic Energy Sciences under contract DE-AC02-76SF00515. The SSRL Structural Molecular Biology Program is supported by the DOE Office of Biological and Environmental Research and by the NIGMS (including P41GM103393). The contents of this publication are solely the responsibility of the authors and do not necessarily represent the official views of the NIGMS, NIAID, or NIH. **Author contributions:** J.A.K., I.A.W., R.H.E.F., R.V., and J.M.W. designed the project; N.S.L., X.Z., R.M.B.H., T.N., J.P., H.L.T., S.M.B., M.J., S.B., J.V., A.V.E., C.T., G.O., and D.Z. performed experiments; J.L. and R.S. performed data analysis; H.V.D., M.P.L., B.B., M.V.D.N.K., L.L.M.P., and A.P.T. designed experiments; and N.S.L., X.Z., A.B.W., B.B., J.A.K., and I.A.W. wrote the manuscript. **Competing interests:** Janssen Vaccines and Prevention has a pending patent application (WO/2016/124768) relating to certain molecules described in this article. **Data and materials availability:** Coordinates and structure factors are deposited in the Protein Data Bank as entries 6FYU, 6FYT, 6CK8, 6FYW, 6FYS, 6CNW, and 6CNV. The EM reconstructions have been deposited in the Electron Microscopy Data Bank under accession code EMD-9029. All other data needed to evaluate the conclusions in this paper are present either in the main text or in the supplementary materials.

SUPPLEMENTARY MATERIALS

www.sciencemag.org/content/362/6414/598/suppl/DC1
Material and Methods
Figs. S1 to S16
Tables S1 to S12
References (*31*–*52*)

27 September 2017; accepted 14 September 2018
10.1126/science.aaq0620

Downloaded from http://science.sciencemag.org/ on April 15, 2021

Science

Universal protection against influenza infection by a multidomain antibody to influenza hemagglutinin

Nick S. Laursen, Robert H. E. Friesen, Xueyong Zhu, Mandy Jongeneelen, Sven Blokland, Jan Vermond, Alida van Eijgen, Chan Tang, Harry van Diepen, Galina Obmolova, Marijn van der Neut Kolfschoten, David Zuijdgeest, Roel Straetemans, Ryan M. B. Hoffman, Travis Nieusma, Jesper Pallesen, Hannah L. Turner, Steffen M. Bernard, Andrew B. Ward, Jinquan Luo, Leo L. M. Poon, Anna P. Tretiakova, James M. Wilson, Maria P. Limberis, Ronald Vogels, Boerries Brandenburg, Joost A. Kolkman and Ian A. Wilson

Science **362** (6414), 598-602.
DOI: 10.1126/science.aaq0620

Durable influenza protection

Vaccines are indispensable for the control and prevention of influenza, but there are several challenges to efficacy. Some individuals respond poorly to vaccination, and virus variation makes targeting optimal antigens difficult. Broadly neutralizing antibodies are one solution, but they have their own pitfalls, including limited cross-reactivity to both influenza A and B strains and the need for repeated injections. Now, Laursen *et al.* have developed multidomain antibodies with breadth and potency. Administered intranasally to mice with an adeno-associated virus vector, the antibodies provided durable and continuous protection from a panoply of influenza strains.

Science, this issue p. 598

ARTICLE TOOLS http://science.sciencemag.org/content/362/6414/598

SUPPLEMENTARY MATERIALS http://science.sciencemag.org/content/suppl/2018/10/31/362.6414.598.DC1

RELATED CONTENT
http://science.sciencemag.org/content/sci/362/6414/511.full
http://stm.sciencemag.org/content/scitransmed/4/147/147ra114.full
http://stm.sciencemag.org/content/scitransmed/5/185/185ra68.full
http://stm.sciencemag.org/content/scitransmed/2/25/25ra24.full
http://stm.sciencemag.org/content/scitransmed/9/413/eaan5325.full

REFERENCES This article cites 46 articles, 10 of which you can access for free
http://science.sciencemag.org/content/362/6414/598#BIBL

PERMISSIONS http://www.sciencemag.org/help/reprints-and-permissions

Use of this article is subject to the Terms of Service

Science (print ISSN 0036-8075; online ISSN 1095-9203) is published by the American Association for the Advancement of Science, 1200 New York Avenue NW, Washington, DC 20005. The title *Science* is a registered trademark of AAAS.

Copyright © 2018 The Authors, some rights reserved; exclusive licensee American Association for the Advancement of Science. No claim to original U.S. Government Works

Downloaded from http://science.sciencemag.org/ on April 15, 2021